5 min, and stained with 0.2 μg/ml FITC-labeled phalloidin (Sigma, St. Louis, MO), which binds actin filaments for 20 min. After washing, the slides were coversliped and observed under a Zeiss LSM510 confocal microscope (Carl Zeiss, Inc., Thornwood, NY).

Statistical Analysis

Statistical analysis was performed with StatView 4.5 (Abacus Concepts, Inc., Berkeley, CA). The Mann–Whitney *U*-test was applied to compare results between two different groups. Repeated-measures ANOVA was used when comparing the in vitro cell migration and invasiveness in an individual group. Statistical significance was assigned at $P < 0.05$.

RESULTS

NE Cells Have no Effect on the Proliferation of Adenocarcinoma Cells

To investigate whether the NE-10 allograft altered the growth of the LNCaP xenograft in vivo, the allograft was co-transplanted into the contralateral back in athymic mice with the LNCaP xenograft. There was no significant difference in the tumor size of LNCaP xenografts between the mice with NE-10 and those without NE-10 for 10 weeks (Fig. 1A). The supernatant of NE-CS cells (NE medium) did not affect the growth of LNCaP cells in vitro on MTT assay (Fig. 1B), which was consistent with the result of the in vivo study. The levels of serum PSA were 189 ± 86 ng/ml in the mice with NE-10 and 260 ± 287 ng/ml in the mice without NE-10 (mean ± standard deviation), with no significant difference between the two groups. These results indicated that NE cells had no effect on the growth of LNCaP cells in vitro or in vivo.

NE Cells Promote Metastasis of Adenocarcinoma Cells

We examined whether the NE-10 allograft influenced the metastatic ability of LNCaP cells. PSA-positive cells, which indicated LNCaP cells in the lungs, were detected in six of nine mice in the LNCaP-only group, and in five of nine mice in the LNCaP + NE-10 group (Fig. 2A). Although, it has been reported that metastasis from the subcutaneously inoculated LNCaP xenograft is extremely rare if examined by routine histological examination with hematoxylin and eosin staining [12], careful examination by PSA immunostaining detected PSA-positive cells in lungs in the LNCaP-only group. Another set of experiments using a different lot number of LNCaP cells showed similar results (data not shown). The number of the clusters of the PSA-positive cells in the LNCaP + NE-10 group

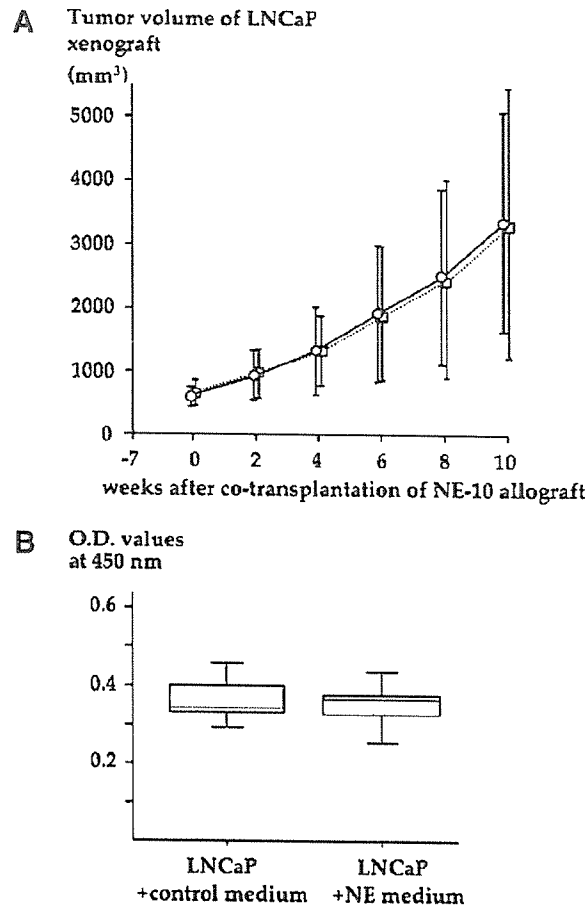

Fig. 1. **A**: Growth rate of LNCaP xenograft in athymic male mice. LNCaP cells (5×10^6) with Matrigel were subcutaneously injected into the backs of 6-week-old athymic mice. At 7 weeks after injection, the mice were randomly divided into two groups (open box, LNCaP-only, n = 9; open circle, LNCaP + NE-10, n = 9). For the LNCaP + NE-10 group, a 50 mg tissue block of the NE-10 allograft was inoculated into the contralateral back in mice with the LNCaP xenograft. Tumor volume (mm^3) is represented as the mean of nine mice in each group. Vertical bars indicate standard deviations. There was no significant difference in the size of the LNCaP xenograft between the two groups. **B**: Proliferation of LNCaP cells in an in vitro study. Cell proliferation was evaluated using MTT assay. There was no significant difference in optical density between LNCaP cells in NE medium and those in control medium ($P = 0.531$, Mann–Whitney *U*-test). Box presents 25th–75th percentiles, as well as median (center line). Bars indicate 5th and 95th percentiles. O.D., optical density.

was significantly greater than that in the LNCaP-only group ($P = 0.012$, Fig. 2B-1). Likewise, the total area of PSA-positive cells per whole lung was significantly larger than that in the LNCaP-only group ($P = 0.012$, Fig. 2B-2). The PSA-positive cells in the LNCaP + NE-10 group were not located adjacent to the Tag-positive cells representing metastases from the NE-10 allograft (Fig. 3).

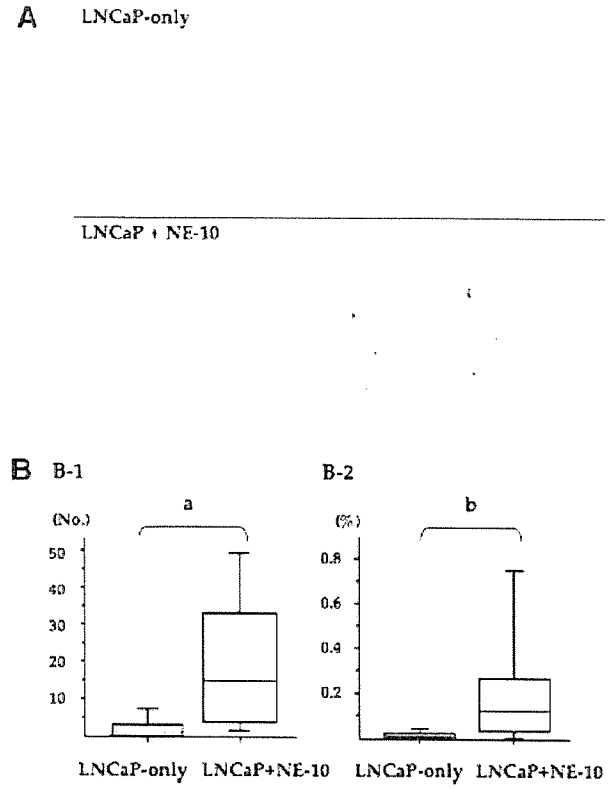

Fig. 2. **A**: Representative NIH images and immunohistochemistry for PSA. The metastatic ability of LNCaP affected by the NE-10 allograft was evaluated in an in vivo study. The LNCaP cells in the lungs of the athymic mice were detected using immunohistochemistry for PSA (**left panels**). Images of PSA-immunostained slides were obtained by digital camera and converted to NIH images (**right panels**). Black areas in NIH images show clusters of PSA-positive cells per unit lung area. Many clusters of PSA-positive cells were observed in the LNCaP + NE-10 group compared to the LNCaP-only group. The clusters of PSA-positive cells in the LNCaP + NE group were generally larger than those of the LNCaP-only group. Reduced from ×200. **B**: Quantitative analysis of the number of clusters of PSA-positive cells (B-1) and the percentage of PSA-positive cells per whole lung section (B-2). The number and percentage of clusters of PSA-positive cells per whole lung section were quantified. The PSA-positive clusters in the LNCaP + NE-10 group were significantly greater in number (B-1) and extent (B-2) than those of the LNCaP-only group (a, $P = 0.012$; b, $P = 0.012$; Mann–Whitney *U*-test). Box presents 25th–75th percentiles, as well as median (center line). Bars indicate 5th and 95th percentiles.

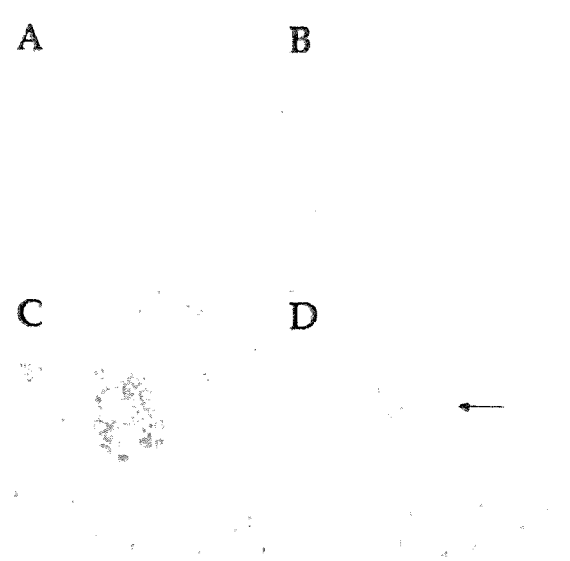

Fig. 3. **A**: Immunohistochemistry for PSA; (**B**) Immunohistochemistry for T-antigen; (**C**) Immunohistochemistry for BrdU; (**D**) Immunohistochemistry for CD31. (A, B, and C were in serial sections). The clusters of PSA-positive cells show positive staining for BrdU. The PSA-positive cells (LNCaP) do not neighbor Tag-positive cells (NE cells). Some clusters of PSA-positive cells lacked CD31-positive endothelial cells (arrow). The results indicated that the PSA-positive cells, which had proliferative activity accompanied by escape from the vascular lumina into the alveoli, were metastases from the LNCaP xenografts that were inoculated into the backs of athymic mice. Reduced from ×400.

We examined whether the PSA-positive cells in the lungs were metastases or just tumor emboli of the cells from the LNCaP xenograft. The nuclei of the PSA-positive cells in serial sections were stained a uniform, dense blue color on BrdU immunohistochemistry without Tag expression (Fig. 3A–C). Immunostaining for CD31 showed that some clusters of PSA-positive cells lacked the surrounding CD31-positive endothelial cells (Fig. 3D). On the other hand, obvious invasion into the alveoli was not detected when the clusters of PSA-positive cells were relatively small. Thus, not all clusters of PSA-positive cells in the lungs were metastases defined as lesions accompanied by escape from the vascular lumina into the alveoli in the present study. However, if we maintained the mice for more than 17 weeks after the inoculation of LNCaP cells, the small tumor emboli that are prerequisite for metastatic development might have become apparent metastases as their tumor size increased since the PSA-positive cells in the lungs had proliferative ability and LNCaP cells possessed invasive potential and could enter into the vascular circulation at the subcutaneously inoculated primary site. Furthermore, it was unlikely that mechanical destruction of the pulmonary tissues by NE-10 metastasis provided a scaffold for LNCaP metastasis because no Tag-positive cells (NE-10 cells) were observed around the metastatic nodules of LNCaP. Thus, the NE-10 allograft promoted pulmonary metastasis of the subcutaneously inoculated LNCaP xenograft.

NE Cells Accelerate the In Vitro Invasion and Migration of Adenocarcinoma Cells, but Not Cell Adhesion

To identify the mechanism by which NE-10 promoted metastasis of LNCaP, we assessed the effect of NE cells on the migration and invasion of LNCaP cells using a Boyden chamber assay. When NE medium was added to the upper chamber with LNCaP cells (Experiment 1), the number of LNCaP cells penetrating through the porous filter without Matrigel coating was significantly greater than that of LNCaP cells in control medium at each given point (Fig. 4A-1). Likewise, when the LNCaP cells were co-cultured with NE-CS cells in the lower chamber (Experiment 2), the number of penetrating LNCaP cells significantly increased (Fig. 4A-2). These results indicated that NE cells enhanced the migration of LNCaP cells. Similarly, the number of LNCaP cells that invaded through the filter with Matrigel significantly increased in the NE medium (Fig. 4B-1, Experiment 1) and in cocultured with NE-CS cells (Fig. 4B-2, Experiment 2), suggesting that NE cells enhanced the invasion of LNCaP cells. Thus, it was speculated that secretions from the NE-CS cells might enhance the migration and in vitro invasion of LNCaP cells. In contrast, the cell adhesion on collagen type IV did not significantly differ between the LNCaP cells with and without NE medium (Fig. 4C). Therefore, the NE-10 allograft promoted pulmonary metastasis of LNCaP cells through enhancement of invasion by facilitating their migration. On the other hand, NE cells had no effect on the proliferation and adhesion to the extracellular matrix of LNCaP cells.

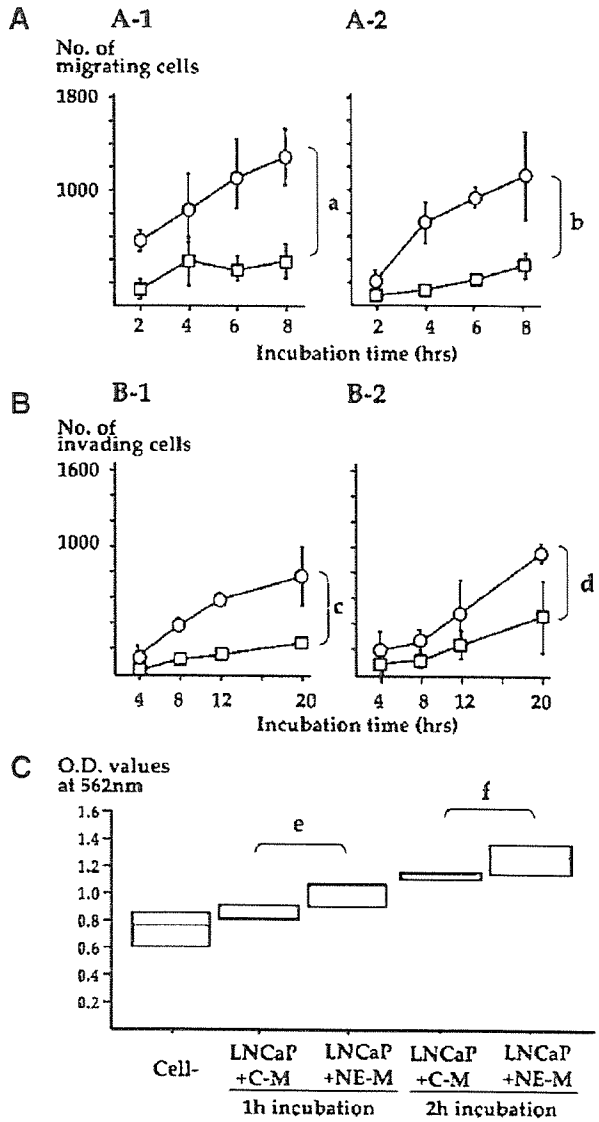

NE Cells Increase the RNA Expression of Eight Genes of Adenocarcinoma Cells That Include the Actin-Regulating Protein Gelsolin

We examined which genes in LNCaP cells were influenced by treatment with NE medium, using CodeLink™ DNA microarray analysis. The microarray for 10,458 gene profiles detected eight genes with upregulation by NE medium (Table I). Of the eight, we focused on gelsolin since it is an important regulator of actin cytoskeleton dynamics required for cell migration. The expression of mRNA of gelsolin was increased by NE medium 1.9- and 1.5-fold at 4 hr and 8 hr, respectively (Fig. 5A). The increased expression of gelsolin induced by NE medium was confirmed using

Fig. 4. **A**: Migration of LNCaP cells. Cell migration assay was performed using a porous filter without Matrigel coating. In Experiment 1 (A-1), 1×10^5 of LNCaP cells were placed into the upper chamber of a Boyden chamber with NE medium (open circle) or control medium (open square). In Experiment 2 (A-2), culture medium with (open circle) or without NE-CS cells (open square) was incubated in the lower chamber for 36 hr and then LNCaP cells suspended in culture medium were placed into the upper chamber. The NE-CS cells significantly facilitated the migration of LNCaP cells (a, $P = 0.005$; b, $P < 0.001$; repeated-measures ANOVA). Vertical bars indicate standard deviations of triplicate experiments. **B**: In vitro invasion of LNCaP cells. Invasion assay was performed using a porous filter with Matrigel coating. Protocols of experiments 1 (B-1) and 2 (B-2) were the same as those for the cell migration assay. The NE-CS cells significantly enhanced the invasion of LNCaP cells (c, $P < 0.001$; d, $P < 0.001$; repeated-measures ANOVA). Vertical bars indicate standard deviations of triplicate experiments. **C**: Adhesion of LNCaP cells. LNCaP cells (1×10^3) were seeded onto wells coated with collagen type IV and incubated at 37°C for 1 hr and two hr. NE medium did not significantly stimulate the adhesion of LNCaP cells (e, $P = 0.191$; f, $P = 0.239$; Mann–Whitney U-test). Box presents 25th–75th percentiles, as well as median (center line) of triplicate experiments. O.D., optical density; C-M, control medium; NE-M, NE medium.

TABLE I. Genes Significantly Overexpressed in LNCaP Cells

ACC[a]	Gene name	Expression ratio 4 hr	Expression ratio 8 hr
AB020716	KIAA0909 Protein	1.6	1.6
NM_000177	Gelsolin	1.9	1.5
NM_003004	Secreted and transmembrane 1 (SECTM1)	2.1	1.6
NM_005224	Dead ringer-like 1 (Drosophila) (DRIL1)	2.0	1.9
NM_005889	Apolipoprotein B mRNA editing enzyme, catalytic polypeptide 1 (APOBEC1), transcript variant 2	1.5	1.8
NM_015196	KIAA0922 protein	1.6	1.5
NM_018321	Hypothetical protein FLJ11100 (FLJ11100)	1.5	1.7
NM_021270	LE hypothetical protein FLJ11100 (FLJ11100) leukocyte-associated IG-like receptor 2 (LAIR2), transcript variant 2	1.9	1.5

Genes with an expression ratio >1.5 were considered to be significantly overexpressed.
[a]GeneBank accession number.

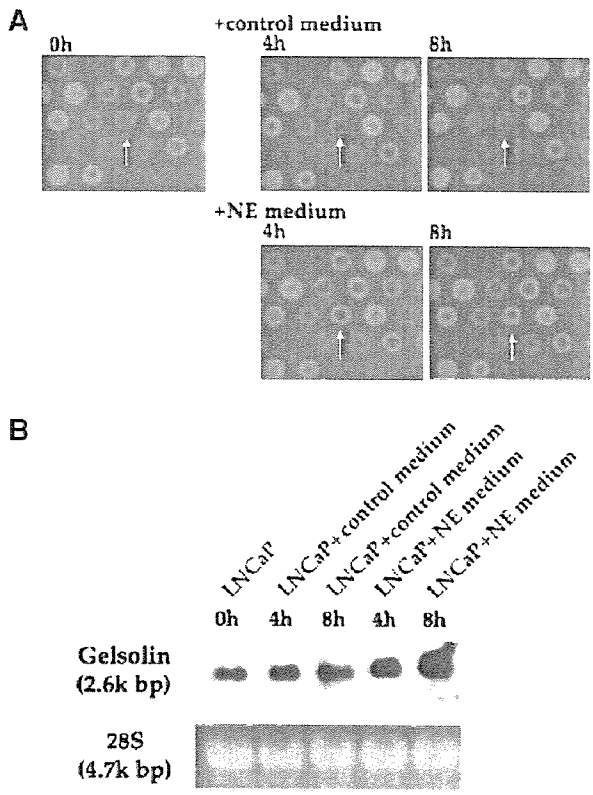

Fig. 5. **A**: Images of DNA microarrays including gelsolin spots in LNCaP cells. The slides show several spots stained with Cy5-streptavidin conjugate (red circles). LNCaP cells with NE medium show prominent signal intensity for gelsolin (arrow) compared to those with control medium at 4 and 8 hr incubation. **B**: Northern blot analysis of mRNA of gelsolin in LNCaP cells. Northern blot analysis demonstrates markedly increased expression of gelsolin in LNCaP cells with NE medium compared to control medium.

Northern blot analysis (Fig. 5B). Thus, it was speculated that the upregulation of gelsolin in LNCaP cells by secretions from NE cells was involved in facilitation of migration of LNCaP cells.

NE Cells Change the Morphology of Adenocarcinoma Cells

We analyzed how NE medium influenced the actin filament dynamics in LNCaP cells. It increased the proportion of LNCaP cells with obvious protrusions (Fig. 6). The conversion of the actin filaments occurred at the bases of protrusions of LNCaP cells. These results suggested that the morphology of LNCaP cells was changed by treatment with NE medium.

DISCUSSION

Although much progress has recently been made in identifying molecular events leading to the development of prostate cancer, the exact mechanisms underlying the acquisition of androgen independence remain poorly understood [13,14]. The possible mechanisms have been reported to be alternations of the activity, function and specificity of AR by mutation or amplification of the *AR* gene [15,16], and activation of intracellular signal transduction pathways that stimulate AR [17,18]. Thus, the mechanism of androgen independence is multifactorial. In addition, recent reports have posited a role of NE differentiated cells in the progression and androgen independence of prostate cancer [9].

NE cells produce growth factors, including vascular endothelial growth factor and transforming growth factor α, which may stimulate growth and accelerate progression of the surrounding adenocarcinoma cells in a paracrine fashion [19]. In addition, NE cells secrete

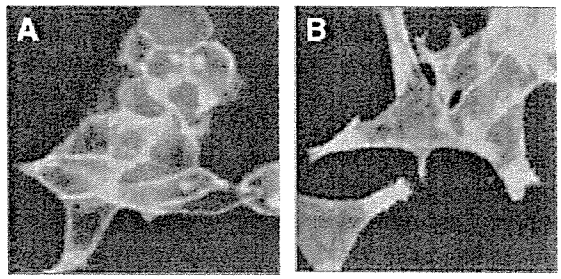

Fig. 6. The LNCaP cells were cultured on fibronectin-coated chamber slides for 6 hr in control medium (**A**) or NE medium (**B**). Filamentous actin was visualized using TRITC-labeled phalloidin under a confocal laser microscope. The LNCaP cells with NE medium possess more prominent protrusions with converting actin filaments at the base than those with control-medium.

a variety of neuropeptides and biogenic amines such as serotonin [1]. It has been clinically reported that the number of NE cells that lack AR increases during androgen ablation therapy [3]. These results indicate that NE cells might play an important role in the development and progression of prostate cancer. However, the prognostic value of NE differentiation is clinically controversial [2,20]. Thus, to investigate the relationship between NE cells and adenocarcinoma cells are mandatory in basic research.

The most critical problem in studying the progression of prostate cancer is the lack of adequate model systems. Although new cell lines and xenografts for human models for NE prostatic carcinoma have been described [21,22], there has been no direct in vivo evidence on whether NE cells influence the development and progression of prostate cancer and androgen independence. Recently, we established the NE-10 allograft and the NE-CS cell line from the ventral prostate of LPB-Tag transgenic mouse line 10 (12T-10) [7,8]. NE-10/NE-CS has the NE property represented by dense core granules in the cytoplasm and androgen-independent growth due to being negative or weakly positive for AR. The development of this NE allograft and NE-CS cell line has provided us with an opportunity to investigate the role of NE cells in prostate cancer.

Previously, we demonstrated that the NE-10 allograft promoted LNCaP tumor growth in castrated mice [9]. In vitro and in vivo studies demonstrated that this effect was mediated by increased AR level/activity in LNCaP cells by NE secretions combined with a low androgen concentration. In the present study, we demonstrated that the NE-10 allograft promoted the metastasis of the LNCaP xenograft in mice having a normal testicular androgen level. The metastatic process consists of multiple steps, including growth at the primary site, invasion into vessels, circulation to the metastatic site, extravasation and growth at distant organs [23]. Cancer cell invasion is a crucial phenomenon for metastasis. It is composed of three steps: cancer cell attachment to the basement membrane, degradation of the extracellular matrix by proteolytic enzymes, and cell migration [24]. We found that the NE-CE cells promoted migration and invasion of LNCaP cells but not cell proliferation and attachment. Thus, it was speculated that the NE cells promoted pulmonary metastasis of LNCaP cells through enhancement of cell invasion by facilitating their migration.

The DNA microarray and Northern blot analysis showed that expression of mRNA of gelsolin in LNCaP cells was increased by the supernatant of NE-CS cells. Gelsolin is an actin-binding protein with well-characterized functions for cytoskeltal reorganization, cell morphology, and motility. Activated gelsolin binds to assembled actin filaments and severs the actin into small fragments (severing). After severing, gelsolin remains attached to the barbed ends of the fragments as a cap to prevent reannealing with each other or elongation at the barbed end (capping). Gelsolin also promotes polymerization of actin monomers to elongate actin filaments (nucleating). Thus, gelsolin mediates the dynamic changes in the actin cytoskeleton for a variety of forms of cell motility [25,26]. In addition, it is known that gelsolin is involved in cellular apoptosis, since it is identified as a substrate of caspase-3 [27]. Gelsolin expression is frequently downregulated in several types of human cancer [28,29], including prostate cancer [30]. Although gelsolin is considered to be a candidate tumor suppressor gene, its role in carcinogenesis remains unclear. Recently, it has been reported that higher expression of gelsolin is associated with a higher risk of recurrence in early stage non-small cell lung cancer and breast cancer [31,32]. In a study on urothelial carcinoma, Rao et al. [33] reported that gelsolin expression decreased in carcinoma in situ and dysplastic lesions compared to benign areas, whereas it gradually increased as the grade and stage became higher. They also demonstrated that higher expression of gelsolin was an independent predictor for recurrence and progression.

In vitro studies have shown that increased expression of gelsolin in cultured fibroblasts results in an increase of cell migration [34,35]. Similarly, it has been demonstrated that overexpression of gelsolin promotes invasion of epithelial cells (MDCK and HEK293T cells) [36]. In the present study, NE cells facilitated the migration of LNCaP cells and increased expression of gelsolin mRNA in LNCaP cells. We also observed that the NE cells enhanced remodeling of the cytoskeletal organization of LNCaP cells. Based upon our evidence and previous studies, it is likely that gelsolin plays an important role in LNCaP tumor cell motility and

invasion, although further study is mandatory to confirm the relationship between upregulation of gelsolin and cell motility in our model.

Nishimura et al. [37] reported that androgen ablation increased the expression of gelsolin in LNCaP cells. The increasing expression of gelsolin enhanced the AR activity under low androgen level, which suggested that gelsolin contributed in maintaining a functional AR signaling pathway even in a low androgen environment. Thus, gelsolin may have a biphasic function in the carcinogenesis and progression of prostate cancer. Expression of gelsolin may be downregulated in the early stage of carcinogenesis, but may later switch to upregulation and promote metastasis by facilitating tumor cell motility. The surrounding NE cells may contribute to upregulation of mRNA of gelsolin in adenocarcinoma cells as well as a change in the characteristics of adenocarcinoma cells per se by androgen ablation since androgen ablation induces LNCaP cells to transdifferentiate into an NE-like phenotype [38]. Our previous study also demonstrated that NE secretions activated AR of LNCaP cells under low androgen levels [9]. Gelsolin, which is upregulated by ablation of testicular androgens may be involved in the development of hormone-refractory prostate cancer where the cancer can respond to low levels of adrenal androgens.

There are several limitations to this study. The NE-10 allograft and the NE-CS cell line, which were derived from the mouse prostate, are of different origin from human adenocarcinoma cell line LNCaP. The role of human NE cells in human prostate cancer may not be the same as mouse NE cells. In addition, the characteristics of the established cell line, NE-CS could be different from those of the original NE-10 allograft because cells suitable for survival in vitro were selected during establishment of the cell line. Thus, peptides or amines secreted from NE cells may be different in NE-10 allograft and NE-CS cells. There are no ideal human lines for which both in vitro and in vivo NE models are available. In addition, it is unknown which factors secreted from NE cells are involved in increased expression of gelsolin. Because NE-10/NE-CS produces several neuropeptides such as chromogranin A, serotonin, and somatostatin, it will be necessary to investigate if these or other factors are crucial for upregulation of gelsolin in LNCaP cells.

Although we need to generate further evidence about the importance of the interaction between adenocarcinoma cells and NE cells in the field of prostate cancer, our results establish a significant role for NE cells in vivo. Learning how to target NE cells may lead to a breakthrough in controlling progression of prostate cancer to metastasis and becoming hormone refractory to androgen ablation treatment.

REFERENCES

1. di Sant'Agnese PA. Neuroendocrine differentiation in carcinoma of the prostate. Diagnostic, prognostic, and therapeutic implications. Cancer 1992;70:254–268.
2. Abrahamsson PA. Neuroendocrine differentiation in prostatic carcinoma. Prostate 1999;39:135–148.
3. Jiborn T, Bjartell A, Abrahamsson PA. Neuroendocrine differentiation in prostatic carcinoma during hormonal treatment. Urology 1998;51:585–589.
4. Casella R, Bubendorf L, Sauter G, Moch H, Mihatsch MJ, Gasser TC. Focal neuroendocrine differentiation lacks prognostic significance in prostate core needle biopsies. J Urol 1998;160:406–410.
5. Abrahamsson PA, Cockett AT, di Sant'Agnese PA. Prognostic significance of neuroendocrine differentiation in clinically localized prostatic carcinoma. Prostate 1998;8:37–42.
6. Masumori N, Thomas TZ, Chaurand P, Case T, Paul M, Kasper S, Caprioli RM, Tsukamoto T, Shappell SB, Matusik RJ. A probasin-large T antigen transgenic mouse line develops prostate adenocarcinoma and neuroendocrine carcinoma with metastatic potential. Cancer Res 2001;61:2239–2249.
7. Masumori N, Tsuchiya K, Tu WH, Lee C, Kasper S, Tsukamoto T, Shappell SB, Matusik RJ. An allograft model of androgen independent prostatic neuroendocrine carcinoma derived from a large probasin promoter-T antigen transgenic mouse line. J Urol 2004;171:439–442.
8. Uchida K, Masumori N, Takahashi A, Itoh N, Tsukamoto T. Characterization of prostatic neuroendocrine cell line established from neuroendocrine carcinoma of transgenic mouse allograft model. Prostate 2005;62:40–48.
9. Jin RJ, Wang Y, Masumori N, Ishii K, Tsukamoto T, Shappell SB, Hayward SW, Kasper S, Matusik RJ. NE-10 neuroendocrine cancer promotes the LNCaP xenograft growth in castrated mice. Cancer Res 2004;64:5489–5495.
10. Albini A, Iwamoto Y, Kleinman HK, Martin GR, Aaronson SA, Kozlowski JM, McEwan RN. A rapid in vitro assay for quantitating the invasive potential of tumor cells. Cancer Res 1987;47:3239–3245.
11. Dorris DR, Ramakrishnan R, Trakas D, Dudzik F, Belval R, Zhao C, Nguyen A, Domanus M, Mazumder A. A highly reproducible, linear, and automated sample preparation method for DNA microarrays. Genome Res 2002;12:976–984.
12. Lim DJ, Liu XL, Sutkowski DM, Braun EJ, Lee C, Kozlowski JM. Growth of an androgen-sensitive human prostate cancer cell line, LNCaP, in nude mice. Prostate 1993;22:109–118.
13. Nelson WG, De Marzo AM, Isaacs WB. Prostate cancer. N Engl J Med 2003;349:366–381.
14. Grossmann ME, Huang H, Tindall DJ. Androgen receptor signaling in androgen-refractory prostate cancer. J Natl Cancer Inst 2001;93:1687–1697.
15. Taplin ME, Bubley GJ, Shuster TD, Frantz ME, Spooner AE, Ogata GK, Keer HN, Balk SP. Mutation of the androgen-receptor gene in metastatic androgen-independent prostate cancer. N Engl J Med 1995;332:1393–1398.
16. Thompson J, Hyytinen ER, Haapala K, Rantala I, Helin HJ, Janne OA, Palvimo JJ, Koivisto PA. Androgen receptor mutations in high-grade prostate cancer before hormonal therapy. Lab Invest 2003;83:1709–1713.
17. Craft N, Shostak Y, Carey M, Sawyers CL. A mechanism for hormone-independent prostate cancer through modulation of androgen receptor signaling by the HER-2/neu tyrosine kinase. Nat Med 1999;5:280–285.

18. Gioeli D, Mandell JW, Petroni GR, Frierson HF Jr, Weber MJ. Activation of mitogen-activated protein kinase associated with prostate cancer progression. Cancer Res 1999;59:279–284.
19. Harper ME, Glynne-Jones E, Goddard L, Thurston VJ, Griffiths K. Vascular endothelial growth factor (VEGF) expression in prostatic tumours and its relationship to neuroendocrine cells. Br J Cancer 1996;74:910–916.
20. di Sant'Agnese PA. Neuroendocrine differentiation in prostatic carcinoma: An update. Prostate 1998;8:74–79.
21. Pinthus JH, Waks T, Schindler DG, Harmelin A, Said JW, Belldegrun A, Ramon J, Eshhar Z. WISH-PC2: A unique xenograft model of human prostatic small cell carcinoma. Cancer Res 2000;60:6563–6567.
22. Okada H, Shirakawa T, Miyake H, Gotoh A, Fujisawa M, Arakawa S, Kamidono S. Establishment of a prostatic small-cell carcinoma cell line (SO-MI). Prostate 2003;56:231–238.
23. Fidler IJ. Critical factors in the biology of human cancer metastasis. Cancer Res 1990;50:6130–6138.
24. Liotta LA. Tumor invasion and metastases- role of the extracellular matrix. Cancer Res 1986;46:1–7.
25. Kwiatkowski DJ. Functions of gelsolin: Motility, signaling, apoptosis, cancer. Curr Opin Cell Biol 1999;11:103–108.
26. Sun HQ, Yamamoto M, Mejillano M, Yin HL. Gelsolin, a multifunctional actin regulatory protein. J Biol Chem 1999;274: 33179–33182.
27. Kothakota S, Azuma T, Reinhard C, Klippel A, Tang J, Chu K, McGarry TJ, Kirschner MW, Koths K, Kwiatkowski DJ, Williams LT. Caspase-3-generated fragment of gelsolin: Effector of morphological change in apoptosis. Science 1997;278:294–298.
28. Asch HL, Head K, Dong Y, Natoli F, Winston JS, Connolly JL, Asch BB. Widespread loss of gelsolin in breast cancers of humans, mice, and rats. Cancer Res 1996;56:4841–4845.
29. Tanaka M, Mullauer L, Ogiso Y, Fujita H, Moriya S, Furuuchi K, Harabayashi T, Shinohara N, Koyanagi T, Kuzumaki N. Gelsolin: A candidate for suppressor of human bladder cancer. Cancer Res 1995;55:3228–3232.
30. Lee HK, Driscoll D, Asch H, Asch B, Zhang PJ. Downregulated gelsolin expression in hyperplastic and neoplastic lesions of the prostate. Prostate 1999;40:14–19.
31. Shieh DB, Godleski J, Herndon JE 2nd, Azuma T, Mercer H, Sugarbaker DJ, Kwiatkowski DJ. Cell motility as a prognostic factor in Stage I nonsmall cell lung carcinoma: The role of gelsolin expression. Cancer 1999;85:47–57.
32. Thor AD, Edgerton SM, Liu S, Moore DH 2nd, Kwiatkowski DJ. Gelsolin as a negative prognostic factor and effector of motility in erbB-2-positive epidermal growth factor receptor-positive breast cancers. Clin Cancer Res 2001;7:2415–2424.
33. Rao J, Seligson D, Visapaa H, Horvath S, Eeva M, Michel K, Pantuck A, Belldegrun A, Palotie A. Tissue microarray analysis of cytoskeletal actin-associated biomarkers gelsolin and E-cadherin in urothelial carcinoma. Cancer 2002;95:1247–1257.
34. Cunningham CC, Stossel TP, Kwiatkowski DJ. Enhanced motility in NIH 3T3 fibroblasts that overexpress gelsolin. Science 1991;251:1233–1236.
35. Azuma T, Witke W, Stossel TP, Hartwig JH, Kwiatkowski DJ. Gelsolin is a downstream effector of rac for fibroblast motility. EMBO J 1998;17:1362–1370.
36. De Corte V, Bruyneel E, Boucherie C, Mareel M, Vandekerckhove J, Gettemans J. Gelsolin-induced epithelial cell invasion is dependent on Ras-Rac signaling. EMBO J 2002;21:6781–6790.
37. Nishimura K, Ting HJ, Harada Y, Tokizane T, Nonomura N, Kang HY, Chang HC, Yeh S, Miyamoto H, Shin M, Aozasa K, Okuyama A, Chang C. Modulation of androgen receptor transactivation by gelsolin: A newly identified androgen receptor coregulator. Cancer Res 2003;63:4888–4894.
38. Burchardt T, Burchardt M, Chen MW, Cao Y, de la Taille A, Shabsigh A, Hayek O, Dorai T, Buttyan R. Transdifferentiation of prostate cancer cells to a neuroendocrine cell phenotype in vitro and in vivo. J Urol 1999;162:1800–1805.

International Journal of Urology (2006) **13**, 951–955

Original Article

Maximum tumor diameter is a simple and valuable index associated with the local extent of disease in clinically localized prostate cancer

RYUICHI MIZUNO,[1] JUN NAKASHIMA,[1] MAKIO MUKAI,[2] HAJIME OOKITA,[2] KEN NAKAGAWA,[1] MOTOTSUGU OYA,[1] TAKASHI OHIGASHI,[1] KEN MARUMO[1] AND MASARU MURAI[1]

[1]*Department of Urology, School of Medicine, Keio University, and* [2]*Division of Diagnostic Pathology, Keio University Hospital, Tokyo, Japan*

Background: The present study was undertaken to investigate the association of pathological features, including the total tumor volume (TTV), maximum tumor area (MTA), and maximum tumor diameter (MTD), with the local extent of disease in clinically localized prostate cancer.

Methods: Serial whole sections of the prostate from 164 patients who underwent radical prostatectomy for localized prostate cancer were investigated. The correlations between the indicators of tumor size, including the TTV, MTA, and MTD, and other pathological parameters were evaluated.

Results: The MTD, MTA, and TTV were significantly correlated with each other. Multivariate stepwise logistic regression analysis indicated that the Gleason score, perineural invasion, microvascular invasion, and MTD were significant independent parameters associated with extraprostatic disease.

Conclusion: The histological tumor grade, perineural invasion, microvascular invasion, and tumor size were correlated with the local extent of disease. The MTD, a simple, easy, and inexpensive parameter, is a more significant pathological feature associated with the local extent of disease than the MTA or TTV.

Key words extraprostatic disease, pathological stage, prostate cancer, tumor diameter, tumor volume.

Introduction

For patients with clinically localized prostate cancer, one of the standard treatments is radical prostatectomy. Despite current staging modalities, including digital rectal examination (DRE), preoperative serum prostate-specific antigen (PSA), transrectal ultrasound (TRUS), pelvic computed tomography (CT), and radionucleotide bone scanning, 26–68% of patients are found to have extraprostatic disease. Patients with extraprostatic disease have a high risk of PSA recurrence after radical prostatectomy.[1] In contrast, patients with organ-confined prostate cancer on pathological examination have a low risk of PSA recurrence after radical prostatectomy.[2] Thus, it is obvious that extraprostatic disease is biologically more aggressive compared with organ-confined disease. Therefore, exploring the pathological features of extraprostatic disease seems valuable for evaluating the biological aggressiveness of prostate cancer.[3–7] The pathological assessment of radical prostatectomy specimens can identify the local extent of disease. Among those postoperative parameters, such as primary Gleason grade, Gleason score, margin status, vascular/lymphatic invasion, perineural invasion, and tumor size, the tumor volume has particularly been considered to be a major determinant of the biological behavior of prostate cancer.[8] There are several different ways of estimating the size of the tumor from radical prostatectomy specimens, including the estimation of the percentage of cancer tissue and image analysis estimation of tumor volume.[9] Although the tumor volume is a good candidate for predicting tumor aggressiveness, its calculation requires much effort and is time-consuming. Therefore, an alternative method of estimating tumor size is desirable.

The present study was undertaken to investigate the significant postoperative pathological features correlated with the local extent of disease and to identify a simple method to replace tumor volume for evaluation of the aggressiveness of clinically localized prostate cancer.

Correspondence: Ryuichi Mizuno, MD, Department of Urology, School of Medicine, Keio University, 35 Shinanomachi, Shinjuku-ku, Tokyo 160-8582, Japan.
Email: mi-zu-no@mub.biglobe.ne.jp

Received 3 February 2004; accepted 12 December 2005.

Methods

Included in this study were 164 cases, ranging in age from 52–74 (mean = 65.9) years, from July 1997 to September 2001. The preoperative serum PSA ranged from 1.6–53.6 (mean = 12.5). The Gleason scores in biopsy specimens ranged from 3–9 (mean = 4.8). All patients underwent a radical prostatectomy at our institution. Prostate cancer

was histologically confirmed preoperatively by TRUS-guided needle biopsy using a 10-MHz endorectal transducer. Indications for prostate biopsy were an abnormal DRE and/or a serum PSA > 4.0 ng/mL. All of the patients underwent a 6-core peripheral zone biopsy protocol at the first screening round and a 12-core peripheral and transition zone biopsy protocol at the second screening round with additional cores from each suspicious area detected by TRUS. The clinical stage was assessed by DRE, abdominal and pelvic CT scans, endorectal magnetic resonance imaging (MRI), and bone scanning. All endorectal MRI studies were performed > 4 weeks after the prostate biopsy to reduce postbiopsy artifact. Tumors that were attached to the prostate capsule and were > 1 cm in width in the endorectal MRI were defined as a subgroup of suspected extension, while tumors with a contact length < 1 cm were defined as a subgroup of no extension.[10] The radical prostatectomy specimens were examined by a single pathologist using fixed and paraffin-embedded sections. The entire specimen was serially blocked at 4-mm intervals with a knife. The specimens were excluded from the study if neoadjuvant hormone therapy or radiation therapy had been performed.

The tumors were graded according to the Gleason grading system. Extracapsular extension (ECE) was defined as a tumor extending outside of the prostate into the periprostatic soft tissues, so tumor invasion of the prostatic capsule without penetration was not ECE. Seminal vesicle invasion (SVI) was diagnosed when the tumor penetrated the muscular coat of the seminal vesicles. Perineural invasion was diagnosed when tumor extension along the perineural sheath was recognized. Microvascular invasion was diagnosed when the tumor penetrated endothelial-lined spaces. We did not differentiate the lymphatics from the blood vessels as making a distinction between them is difficult in the prostate. The tumor border was outlined on the coverslip of the slide using a marking pen. The maximum diameter of the largest single tumor focus was determined by marking both ends of the lesion with a pen and measuring this distance directly on the glass slide with a ruler. The tumor area on each slide was measured with commercially available software. The volume of each cancer was calculated as the sum of the surface areas for that tumor multiplied by the thickness of the prostate slice. The maximum tumor diameter (MTD) *in vivo* was estimated by multiplying the measured maximum diameter by a factor of 1.1 to correct for tissue shrinkage during formalin fixation and embedding in paraffin. The maximum tumor area (MTA) *in vivo* was corrected by a factor of 1.21 and the total tumor volume (TTV) was corrected by a factor of 1.33.

The Spearman's rank correlation test was used to evaluate the correlations between the variables. The variables for different groups were compared using the Mann–Whitney *U*-test. The independence of fit of the categorical data was analyzed by the χ^2-test. Independent factors for the prediction of extraprostatic cancer were identified by stepwise logistic regression analyses. The differences were considered statistically significant at $P < 0.05$ and the results are presented as the mean ± standard error.

Results

Pathologically, 105 men (64.0%) had disease confined to the prostate and 59 (36.0%) had extraprostatic disease. Among the 59 cases of extraprostatic disease, ECE was seen in 54 cases (32.9%) and 10 (6.1%) had SVI. Microvascular invasion was seen in 45 cases (27.4%). Perineural invasion was observed in 119 patients (72.6%). The primary Gleason grade ranged from 2–5 (mean = 3.1). The Gleason scores ranged from 3–9 (mean = 6.1). The MTD ranged from 0.46–4.83 cm (mean = 2.04), the MTA ranged from 0.10–10.92 cm^2 (mean = 1.80), and the TTV ranged from 0.05–33.30 cm^3 (mean = 3.96).

The results of the Spearman's rank correlation analyses are shown in Figure 1. The MTD was significantly correlated with the TTV ($r = 0.708$, $P < 0.0001$), as well as with the MTA ($r = 0.814$, $P < 0.0001$). The MTA was significantly correlated with the TTV ($r = 0.918$, $P < 0.0001$) (Fig. 1). The TTV ($r = 0.309$, $P < 0.0001$), MTA ($r = 0.289$, $P = 0.0002$), and MTD ($r = 0.332$, $P = 0.0004$) all increased with an increase of the Gleason score and were significantly correlated with this score (Fig. 2). The TTV, MTA, and MTD were significantly greater in patients with microvascular invasion (5.62 ± 0.82 cm^3, 2.42 ± 0.27 cm^2, and 2.41 ± 0.13 cm, respectively) or perineural invasion (4.57 ± 0.41 cm^3, 2.03 ± 0.14 cm^2, and 2.25 ± 0.08 cm, respectively) than in those without microvascular invasion (3.33 ± 0.33 cm^3, 1.56 ± 0.12 cm^2, and 1.91 ± 0.08 cm, respectively) and those without perineural invasion (2.35 ± 0.54 cm^3, 1.16 ± 0.19 cm^2, and 1.49 ± 0.11 cm, respectively). The TTV, MTA, and MTD were significantly greater in patients with ECE, SVI, and extraprostatic disease than their counterparts (Tables 1–3). The primary Gleason grade, Gleason score, and the incidence of microvascular invasion and perineural invasion were significantly higher in patients with ECE, SVI, or extraprostatic disease than their respective counterparts (Tables 1–3).

In addition, multivariate stepwise logistic regression analysis demonstrated that the MTD ($P = 0.0037$), Gleason score ($P = 0.0355$), microvascular invasion ($P = 0.0333$), and perineural invasion ($P = 0.0217$) showed a significant independent association with ECE (Table 4). Without the MTD, the MTA ($P = 0.0236$), Gleason score ($P = 0.0335$), microvascular invasion ($P = 0.0189$), and perineural invasion ($P = 0.0102$) were significantly correlated with ECE. The TTV ($P = 0.0261$), Gleason score ($P = 0.0498$), microvascular invasion ($P = 0.0151$), and perineural invasion ($P = 0.0086$) were correlated with ECE when the MTD and MTA were removed from the analysis. Multivariate stepwise logistic regression analysis also demonstrated that the MTD ($P = 0.0026$), Gleason score ($P = 0.0088$), microvascular invasion ($P = 0.0028$), and perineural invasion ($P = 0.0195$) had a significant independent association with extraprostatic disease (Table 5). Without the MTD, the MTA ($P = 0.0236$), Gleason score ($P = 0.0335$), microvascular invasion ($P = 0.0189$), and perineural invasion ($P = 0.0102$) were significantly correlated with extraprostatic extension. The TTV ($P = 0.0261$), Gleason score ($P = 0.0498$), microvascular invasion

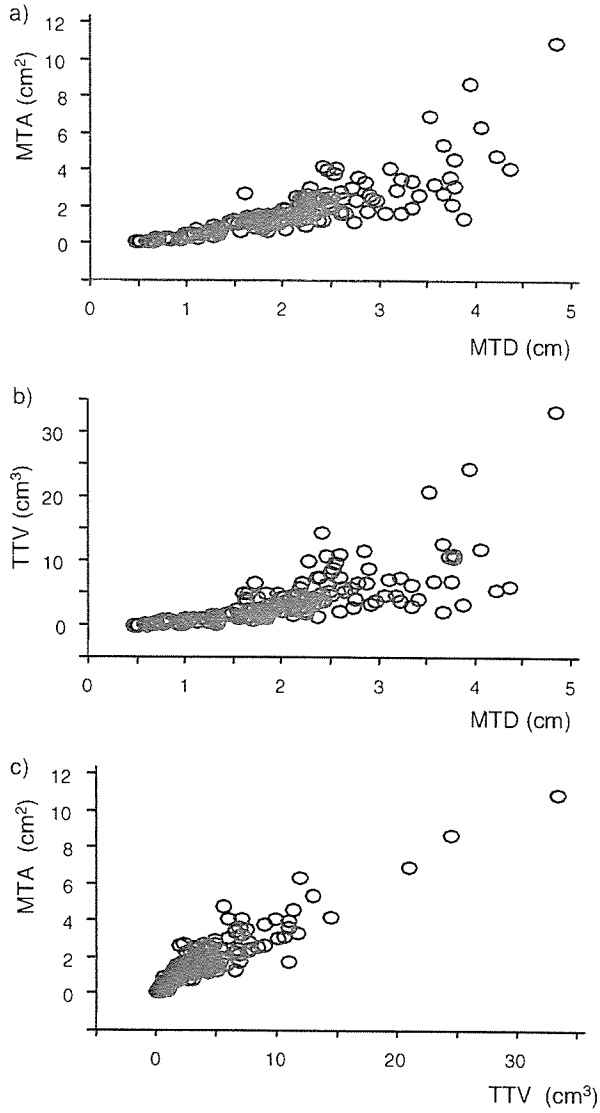

Fig. 1 Correlations between the total tumor volume (TTV), maximum tumor area (MTA), and maximum tumor diameter (MTD) were examined by Spearman's analysis. (a) Correlation between the MTD and MTA ($r = 0.814$, $P < 0.0001$). (b) Correlation between the MTD and TTV ($r = 0.708$, $P < 0.0001$). (c) Correlation between the TTV and MTA ($r = 0.918$, $P < 0.0001$).

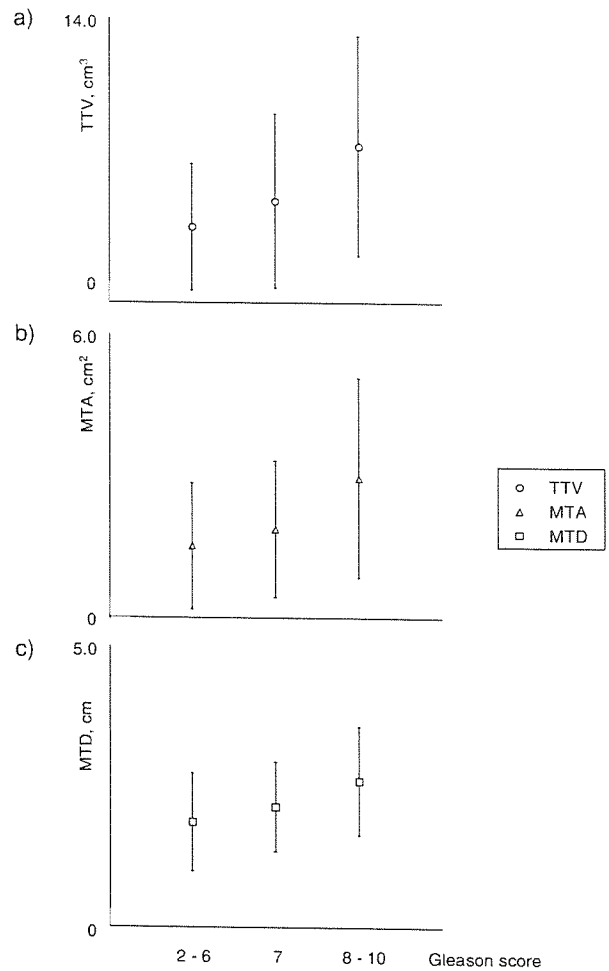

Fig. 2 Correlations between the Gleason score and the total tumor volume (TTV), maximum tumor area (MTA), and maximum tumor diameter (MTD). (a) Correlation between the Gleason score and TTV ($r = 0.309$, $P < 0.0001$). (b) Correlation between the Gleason score and MTA ($r = 0.289$, $P = 0.0002$). (c) Correlation between the Gleason score and MTD ($r = 0.332$, $P = 0.0004$).

($P = 0.0151$), and perineural invasion ($P = 0.0086$) were correlated with extraprostatic extension when the MTD and MTA were removed from the analysis.

Discussion

Extraprostatic disease is an important finding in prostate cancer because of its implications regarding biological activity. Therefore, preoperative staging prior to radical prostatectomy using currently available modalities has been performed.[11] Accordingly, the precise identification of patients with organ-confined prostate cancer as candidates for radical prostatectomy would contribute to the improvement of the survival rate of patients undergoing this surgery. However, some prostatectomy specimens still demonstrate ECE, SVI or extraprostatic disease in those with clinically localized prostate cancer. In the current study, we analyzed postoperative parameters to assess the biological aggressiveness of prostate cancer and found that many of them were significantly correlated with ECE, SVI or extraprostatic disease. In addition, multivariate stepwise logistic regression analyses demonstrated that some postoperative parameters were independent indices in association with ECE or extraprostatic disease.

Among those postoperative parameters, tumor volume is the most commonly used measure of the amount of tumor, which is a well-recognized predictor of biological

Table 1 Association of postoperative pathological parameters with pathological extracapsular extension

Pathological parameter	pECE(−)	pECE(+)	*P*-value
TTV (cm^3)	2.99 ± 0.31	3.96 ± 0.34	<0.0001
MTA (cm^2)	1.45 ± 0.12	2.49 ± 0.24	<0.0001
MTD (cm)	1.81 ± 0.08	2.53 ± 0.11	<0.0001
Primary Gleason score	2.94 ± 0.12	3.49 ± 0.12	<0.0001
Gleason score	5.82 ± 0.12	6.72 ± 0.17	<0.0001
Microvascular invasion	18/110 (15.6%)	27/54 (50.0%)	0.0007
Perineural invasion	69/110 (62.7%)	50/54 (92.6%)	0.0009

MTA, maximum tumor area; MTD, maximum tumor diameter; pECE, pathological extracapsular extension; TTV, total tumor volume.

Table 2 Association of postoperative pathological parameters with pathological seminal vesicle invasion

Pathological parameter	pSVI (−)	pSVI (+)	*P*-value
TTV (cm^3)	3.73 ± 0.34	7.56 ± 1.10	0.0003
MTA (cm^2)	1.72 ± 0.12	2.95 ± 0.32	0.0005
MTD (cm)	2.01 ± 0.71	2.55 ± 0.14	0.0066
Primary Gleason score	3.08 ± 0.05	3.78 ± 0.28	0.0446
Gleason score	6.05 ± 0.10	7.20 ± 0.36	0.0093
Microvascular invasion	38/154 (24.7%)	7/10 (70.0%)	0.0019
Perineural invasion	109/154 (70.8%)	10/10 (100%)	0.0454

MTA, maximum tumor area; MTD, maximum tumor diameter; pSVI, pathological seminal vesicle invasion; TTV, total tumor volume.

Table 3 Association of postoperative pathological parameters with extraprostatic disease

Pathological parameter	Organ-confined	Extraprostatic	*P*-value
TTV (cm^3)	2.88 ± 0.32	5.87 ± 0.69	<0.0001
MTA (cm^2)	1.41 ± 0.12	2.50 ± 0.22	<0.0001
MTD (cm)	1.78 ± 0.08	2.52 ± 0.10	<0.0001
Primary Gleason score	2.93 ± 0.06	3.47 ± 0.10	0.0446
Gleason score	5.74 ± 0.12	6.78 ± 0.16	<0.0001
Microvascular invasion	14/105 (13.3%)	31/59 (52.5%)	<0.0001
Perineural invasion	64/105 (61.0%)	41/59 (69.5%)	<0.0001

MTA, maximum tumor area; MTD, maximum tumor diameter; TTV, total tumor volume.

Table 4 Multivariate logistic regression analysis for the pathological parameters correlated with pathological extracapsular extension

Pathologic parameter	*P*-value	Odds ratio	95% CI
MTD (cm)	0.0037	2.086	1.269–3.429
Gleason score	0.0355	1.431	1.025–1.999
Microvascular invasion	0.0333	2.671	1.154–6.182
Perineural invasion	0.0217	3.578	1.106–11.572

CI, confidence interval; MTD, maximum tumor diameter.

Table 5 Multivariate logistic regression analysis for the pathological parameters correlated with extraprostatic disease

Pathologic parameters	*P*-value	Odds ratio	95% CI
MTD (cm)	0.0026	2.218	1.321–3.724
Gleason score	0.0088	1.599	1.126–2.270
Microvascular invasion	0.0028	3.790	1.582–9.079
Perineural invasion	0.0195	4.203	1.260–14.023

CI, confidence interval; MTD, maximum tumor diameter.

behavior in many organs. In the case of prostate cancer, although the data on tumor volume have been accumulated, it is still not clear whether the volume is an independent predictor of tumor aggressiveness.[12–17] There are several different methods of evaluating the tumor volume in prostate cancer, but accurate measurement is difficult and time-consuming.[18] In this study, we tried to determine a rapid, simple, and objective method for evaluating prostate cancer on the basis of size instead of the tumor volume. Therefore, we measured the area and diameter of the

largest tumor focus on the slide glass. Both methods that we tested seemed to work to some extent, as the TTV, MTA, and MTD were significantly correlated with each other. This result should not be surprising because most small tumors do not possess other foci. We also demonstrated that the TTV, MTA, and MTD showed a significant increase with an advancing Gleason score and were significantly greater in patients with ECE, SVI, and extraprostatic disease than in patients without such findings. Based on these results, we consider that tumor size is correlated with tumor aggressiveness and that its estimation is desirable in patients with prostate cancer. Measuring the MTD is a simple and inexpensive method of evaluating tumor size.

In this study, the TTV, MTA, and MTD demonstrated significant associations with ECE, SVI and extraprostatic disease on univariate analyses. However, multivariate stepwise logistic regression analyses demonstrated that the MTD was a more valuable index than the MTA or TTV in association with locally advanced disease and that the MTD is an independent index of such disease along with the Gleason score, microvascular invasion, and perineural invasion. This strongly suggests that, even though the majority of large tumors is multifocal, the degree of aggressiveness might depend most on the largest focus. As the MTD is along the prostate capsule in many cases, it seems likely that the probability of a tumor demonstrating extraprostatic disease is related to the extent of its presence at the capsular surface. The results in this study imply the possibility of MTD as one of the most important prognostic factors for predicting PSA recurrence after radical prostatectomy. Further studies will be necessary to elucidate the prognostic significance of tumor size, including MTD, MTA, and TTV in the future.

In conclusion, our data demonstrated that the MTD, a simple, easy, and inexpensive parameter, is a more significant pathological feature associated with the local extent of disease than the MTA or TTV.

References

1 Partin AW, Yoo J, Carter HB *et al.* The use of prostate specific antigen, clinical stage and Gleason score to predict pathological stage in men with localized prostate cancer. *J. Urol.* 1993; **150**: 110–14.

2 Han M, Partin AW, Zahurak M, Piantadosi S, Epstein JI, Walsh PC. Biochemical (prostate specific antigen) recurrence probability following radical prostatectomy for clinically localized prostate cancer. *J. Urol.* 2003; **169**: 517–23.

3 Palisaan RJ, Graefen M, Karakiewicz PI *et al.* Assessment of clinical and pathologic characteristics predisposing to disease recurrence following radical prostatectomy in men with pathologically organ-confined prostate cancer. *Eur. Urol.* 2002; **41**: 155–61.

4 Villers A, McNeal JE, Redwine EA, Freiha FS, Stamey TA. The role of perineural space invasion in the local spread of prostatic adenocarcinoma. *J. Urol.* 1989; **142**: 763–8.

5 Bahnson RR, Dresner SM, Gooding W, Becich MJ. Incidence and prognostic significance of lymphatic and vascular invasion in radical prostatectomy specimens. *Prostate* 1989; **15**: 149–55.

6 Salomao DR, Graham SD, Bostwick DG. Microvascular invasion in prostate cancer correlates with pathologic stage. *Arch. Pathol. Lab. Med.* 1995; **119**: 1050–4.

7 McNeal JE, Yemoto CE. Significance of demonstrable vascular space invasion for the progression of prostatic adenocarcinoma. *Am. J. Surg. Pathol.* 1996; **20**: 1351–60.

8 McNeal JE, Bostwick DG, Kindrachuk RA, Redwine EA, Freiha FS, Stamey TA. Patterns of progression in prostate cancer. *Lancet* 1986; **1**: 60–3.

9 Humphrey PA, Vollmer RT. Percentage carcinoma as a measure of prostatic tumor size in radical prostatectomy tissues. *Mod. Pathol.* 1997; **10**: 326–33.

10 Horiguchi A, Nakashima J, Horiguchi Y *et al.* Prediction of extraprostatic cancer by prostate specific antigen density, endorectal MRI, and biopsy Gleason score in clinically localized prostate cancer. *Prostate* 2003; **56**: 23–9.

11 Epstein JI, Partin AW, Sauvageot J, Walsh PC. Prediction of progression following radical prostatectomy. A multivariate analysis of 721 men with long-term follow-up. *Am. J. Surg. Pathol.* 1996; **20**: 286–92.

12 Humphrey PA, Vollmer RT. Intraglandular tumor extent and prognosis in prostatic carcinoma: application of a grid method to prostatectomy specimens. *Hum. Pathol.* 1990; **21**: 799–804.

13 Humphrey PA, Frazier HA, Vollmer RT, Paulson DF. Stratification of pathologic features in radical prostatectomy specimens that are predictive of elevated initial postoperative serum prostate-specific antigen levels. *Cancer* 1993; **71**: 1821–7.

14 McNeal JE, Villers AA, Redwine EA, Freiha FS, Stamey TA. Capsular penetration in prostate cancer. Significance for natural history and treatment. *Am. J. Surg. Pathol.* 1990; **14**: 240–7.

15 Stamey TA, McNeal JE, Freiha FS, Redwine E. Morphometric and clinical studies on 68 consecutive radical prostatectomies. *J. Urol.* 1988; **139**: 1235–41.

16 Epstein JI, Carmichael M, Partin AW, Walsh PC. Is tumor volume an independent predictor of progression following radical prostatectomy? A multivariate analysis of 185 clinical stage B adenocarcinomas of the prostate with 5 years of followup. *J. Urol.* 1993; **149**: 1478–81.

17 Partin AW, Epstein JI, Cho KR, Gittelsohn AM, Walsh PC. Morphometric measurement of tumor volume and per cent of gland involvement as predictors of pathological stage in clinical stage B prostate cancer. *J. Urol.* 1989; **141**: 341–5.

18 Renshaw AA, Chang H, D'Amico AV. Estimation of tumor volume in radical prostatectomy specimens in routine clinical practice. *Am. J. Clin. Pathol.* 1997; **107**: 704–8.

Treatment of localized prostate cancer using high-intensity focused ultrasound

TOYOAKI UCHIDA, HIROSHI OHKUSA, YASUNORI NAGATA, TORU HYODO*, TAKEFUMI SATOH* and AKIRA IRIE*

*Departments of Urology, University of Tokai Hachioji Hospital, Hachioji, and *University of Kitasato, Sagamihara, Japan*

Accepted for publication 12 July 2005

OBJECTIVE

To evaluate the biochemical disease-free survival (DFS), predictors of clinical outcome and morbidity of patients with localized prostate cancer treated with high-intensity focused ultrasound (HIFU), a noninvasive treatment that induces complete coagulative necrosis of a tumour at depth through the intact skin.

PATIENTS AND METHODS

In all, 63 patients with stage T1c-2bN0M0 localized prostate cancer underwent HIFU using the Sonablate™ system (Focus Surgery, Inc., Indianapolis, IN, USA). None of the patients received neoadjuvant and/or adjuvant therapy. Biochemical recurrence was defined according to the criteria recommended by the American Society for Therapeutic Radiology and Oncology consensus definition, i.e. three consecutive increases in prostate-specific antigen (PSA) level after the nadir. The median (range) age, PSA level and follow-up were 71 (45–87) years, 8.5 (3.39–57.0) ng/mL and 22.0 (3–63) months, respectively.

RESULTS

The overall biochemical disease-free rate was 75% (47 patients). The 3-year biochemical DFS rates for patients with a PSA level before HIFU of <10, 10.01–20 and >20 ng/mL were 82%, 62% and 20% ($P < 0.001$), respectively. The 3-year biochemical DFS rates for patients with a PSA nadir of <0.2, 0.21–1 and >1 ng/mL were 100%, 74% and 21% ($P < 0.001$), respectively. Final follow-up sextant biopsies showed that 55 (87%) of the patients were cancer-free. Multivariate analysis showed that the PSA nadir ($P < 0.001$) was a significant independent predictor of relapse.

CONCLUSION

HIFU therapy appears to be a safe, effective and minimally invasive therapy for patients with localized prostate cancer, and the PSA nadir is a useful predictor of clinical outcome.

KEYWORDS

localized prostate cancer, minimally invasive therapy, high-intensity focused ultrasound

INTRODUCTION

Prostate cancer is the most common malignancy in men and the second leading cause of death from cancer in the USA [1]. Radical prostatectomy (RP) has long been regarded as appropriate therapy for patients with organ-confined prostate cancer. Despite excellent 5- and 10-year survival rates after RP, surgery is associated with significant morbidity, e.g. blood loss with transfusion-related complications, erectile dysfunction in 30–70% of men, and stress incontinence in up to 10% [2–5]. In addition, surgical intervention is not typically considered for patients whose life-expectancy is <10 years. Recently, several alternative and less invasive treatments have been developed to treat localized prostate cancer. Brachytherapy, cryosurgical ablation of the prostate, three-dimensional conformal radiotherapy, intensity-modulated external beam radiotherapy and laparoscopic RP have been used [6–10]. However, these alternative treatments, except the conformal radiotherapy and intensity-modulated therapy, require at least percutaneous access.

High-intensity focused ultrasound (HIFU) is a noninvasive technique for the thermal ablation of tissue. HIFU can noninvasively induce complete coagulative necrosis of a target tumour, without requiring surgical exposure or insertion of instruments into the lesion. This advantage makes it one of the most attractive potential options for the localized treatment of tumours. Since January 1999, we have been treating localized prostate cancer with transrectal HIFU [11,12]; we report the efficacy, safety and predictive preoperative values of HIFU ablation for treating patients with localized prostate cancer.

PATIENTS AND METHODS

We used the Sonablate™ (Focus Surgery, Inc., Indianapolis, IN, USA) HIFU machine; the treatment module includes the ultrasound power generator, multiple transrectal probes of different focal depth, the probe-positioning system, and a continuous cooling system (Fig. 1). The transrectal HIFU probes use proprietary transducer technology with low-energy ultrasound (4 MHz) for imaging the prostate and to deliver high-energy ablative pulses (site intensity, 1300–2200 W/cm^2). The single piezoelectric crystal alternates between high-energy power for ablative (3 s) and low-energy for ultrasound imaging (6 s).

Before starting the treatment the operator uses longitudinal and transverse ultrasonograms to obtain an image of the prostate and selects the prostate tissue volume to be ablated by a set of cursors on these images. The probe houses a computer-controlled positioning system, which directs each ablative pulse to the targeted region of the prostate. Each discrete HIFU pulse ablates a volume of 3 × 3 × 10 mm of tissue [13]. The total acoustic power is initially set at 24 and 37 W for 3- and 4-cm focal length probes, respectively. The individual focal lesion produces almost instantaneous coagulative

© 2006 BJU INTERNATIONAL | 97, 56–61 | doi:10.1111/j.1464-410X.2006.05864.x

FIG. 1. The Sonablate-500 device consists of an operator's console, imaging monitor, transrectal probe and an automatic continuous cooling system.

FIG. 2. The computer-controlled transducer ablates the entire prostate tissue. Focal lesions are overlapped in linear rows (left) at each of the lateral sector positions (right), to create a volume lesion.

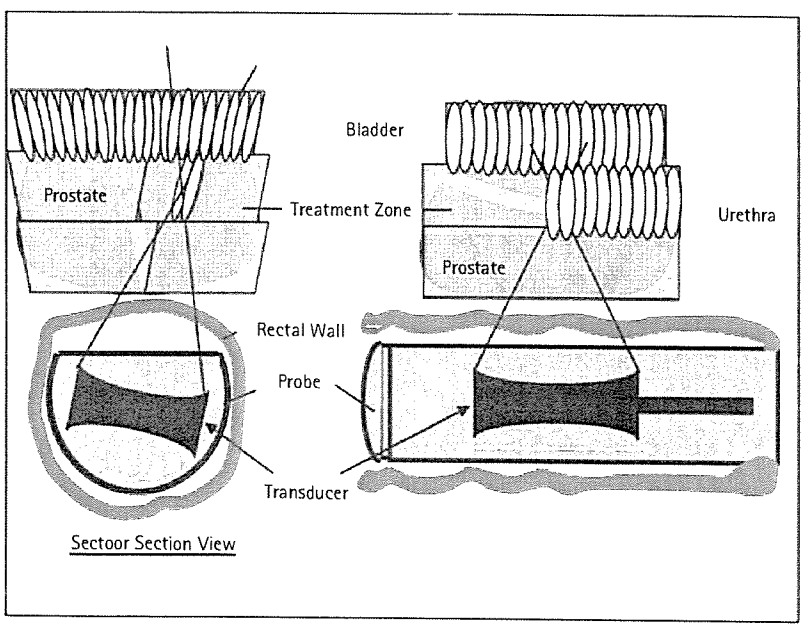

necrosis of tissue as the temperature increases to 80–98 °C in the focal zone [13,14]. Under computer control, the ultrasound beam is steered mechanically to produce consecutive lesions so that all focal lesions overlap laterally and longitudinally to ensure necrosis of the entire targeted prostate volume (Fig. 2). An automatic cooling device is used during treatment to maintain a constant baseline temperature of <18 °C in the transrectal probe, which helps to prevent thermal injury of the rectal mucosa.

All patients were anaesthetized by epidural or spinal anaesthesia, and placed supine with open legs. A condom was placed over the probe and degassed water was used to inflate the condom, which was covered with ultrasound gel for close coupling of the ultrasound probe to the rectal wall, and the probe was inserted manually into the rectum. The probe was fixed in position by an articulating arm attached to the operating table. After selecting the treatment region of the prostate from the verumontanum to the bladder neck, the treatment was started. Transrectal probes with focal lengths of 3.0 and 4.0 cm were used according to the size of the prostate, as determined by TRUS, with larger glands requiring longer focal lengths. The treatment continued layer by layer (10 mm thick) from the apex to the base (Fig. 2). Usually, three successive target areas (anterior, mid-part and base) were defined to treat the whole prostate. After completing the treatment, a transurethral balloon catheter or percutaneous cystostomy was inserted into the bladder.

The study included patients with stage T1c–2bN0M0 localized prostate cancer; those with anal stricture were excluded from the study. None of the patients received adjuvant hormonal and/or chemotherapy. All patients were fully informed of the details of this treatment and provided written consent before HIFU. Beginning in January 1999, 63 patients with clinically localized prostate cancer were treated with HIFU. Evaluations before HIFU included a history, physical examinations, including a DRE, initial PSA level and Gleason score on needle biopsy of the prostate. All patients had a negative radionuclide bone scan and CT of the abdomen and pelvis confirmed that there was no metastatic disease. Tumours were staged using the TNM staging system [15]. The characteristics of the 63 patients are listed in Table 1.

Patient status and treatment-related complications were followed using all available means, including periodic patient visits and self-administered questionnaires on urinary continence and erectile function. The serum PSA level was usually assayed every 1–6 months during the follow-up. At 6 months after HIFU a prostate biopsy was taken in all patients. The American Society for Therapeutic Radiology and Oncology (ASTRO) consensus definition for biochemical failure, i.e. three consecutive increases in PSA level

after a nadir, was used to define biochemical failure [16]. The time to biochemical failure was defined as midway between the PSA nadir and the first of the three consecutive PSA increases. None of the patients received androgen deprivation after HIFU or other anticancer therapy before documentation of a biochemical failure.

The chi-squared test was used to assess the correlation between variables before and after HIFU. Distributions of biochemical disease-free survival (DFS) times were calculated according to the Kaplan-Meier curves and the log-rank test used to determine the differences between the curves. A multivariate Cox proportional hazards regression model was used to estimate the prognostic relevance of age, clinical stage, Gleason score, volume of the prostate, pretreatment and nadir serum PSA levels on DFS, with $P < 0.05$ taken to indicate statistical significance.

RESULTS

The prostate was treated in one (50 patients) or two (13) HIFU sessions for a total of 76 procedures in 63 patients (1.2 sessions/patient). Reasons for repeating the HIFU treatments were: in five patients because we tried different 'on' and/or 'off' times, e.g. shorter (2 s) and/or longer off (8-12 s) intervals before establishing the standard on (3 s) and off (6 s) interval; in three for residual tumour or PSA increases; two were only treated on the right or left lobe of the prostate; two because they had a large prostate; and one because there was a problem with the HIFU machine. The median (range) operative duration and hospitalization was 149 (55-356) min and 4 (2-20) days, respectively. The gland size decreased from an initial mean volume of 28.6 mL to a final median volume of 14.5 mL ($P < 0.001$) in a mean of 6.5 (3-23) months. The mean (SD, median) PSA nadir levels were 1.38 (2.55, 0.5) ng/mL.

Of the 63 patients, 47 (75%) were biochemically disease-free during the follow-up; the 3-year biochemical DFS rates for those with a PSA level before HIFU of <10, 10.01-20 and >20 ng/mL was 82%, 62% and 20%, respectively ($P < 0.001$). The PSA nadir was 4-8 weeks after treatment; the 3-year biochemical DFS rates for patients with a PSA nadir of <0.2 (20 patients), 0.21-1.0 (25) and >1 (18) were 100%, 74% and 21% (log-rank test, $P < 0.001$), respectively. Risk factors were a PSA level of ≥10 ng/mL, a Gleason score of ≥7, and stage T2b disease, with patients at low-risk having none of these factors, at moderate risk having one and at high risk having two or more [17]. The 3-year biochemical DFS rates in patients at low, moderate and high risk was 84%, 69% and 51% ($P = 0.0295$), respectively (Fig. 3). However, there was no statistically significant difference in patients within stage and Gleason score groups.

Characteristic	Value
Mean (SD), median (range):	
Age, years	70.5 (1.3), 71 (45-87)
PSA, ng/mL	11.2 (8.7), 8.5 (3.39-57.0)
Prostate volume, mL	28.5 (11.9), 25.9 (13.2-68.8)
Follow-up, months	23.3 (12.7), 22.0 (3-63)
N (%):	
PSA level (ng/mL) before HIFU	
≤ 10	34 (54)
10.1-20	24 (38)
>20	5 (8)
Clinical stage	
T1c	39 (62)
T2a	18 (29)
T2b	6 (9)
Gleason score	
2-4	13 (21)
5-7	46 (73)
8-10	4 (6)
Risk group	
Low	22 (35)
Intermediate	26 (41)
High	15 (24)
PSA nadir (ng/mL)	
0-0.2	20 (32)
0.21-1.0	25 (40)
>1.0	18 (28)

TABLE 1
The clinicopathological data of 63 patients with localized prostate cancer

In the Cox regression analysis, the PSA nadir was a statistically significant variable for prognosis but age, stage, Gleason grading, serum PSA level and prostate volume were not (Table 2). The final follow-up prostate biopsies showed that 55 (87%) of the 63 patients were cancer-free. The main pathological findings of the prostate biopsy at 6 months after HIFU showed a coagulation necrosis and fibrosis.

All patients reported urinary symptoms, e.g. frequency, urgency and difficulty in urination, during the first 2 months after HIFU treatment. The symptoms were transitory and easily managed by medical treatment. Urethral catheters in all patients were removed 1-2 days after HIFU, but were reinserted in those who could not urinate spontaneously, and removal was attempted every 1-2 weeks thereafter. The median (range) urinary catheterization period after HIFU was 14 (0-31) days. Fifteen (24%) patients developed a urethral stricture, two (3%) complained of retrograde ejaculation and two (3%) other patients of epididymitis. One (2%) patient had a TURP for prolonged urinary retention, one (2%) had grade 1 transient incontinence for a month, and one (2%) developed a recto-urethral fistula (Table 3). Eight of the 34 patients who were sexually active complained of erectile dysfunction after HIFU; two of these eight who desired treatment were treated with sildenafil citrate, and recovered.

DISCUSSION

In 1995, Madersbacher *et al.* [14] reported the effect of HIFU (using the older Sonablate 200 system) in an experimental study of 10 patients with histologically confirmed hypoechoic and palpable localized prostate

FIG. 3. Kaplan–Meier biochemical disease-free survival curves according to: a, stage; b, Gleason score; c, serum PSA level; d, risk group; and e, PSA nadir level.

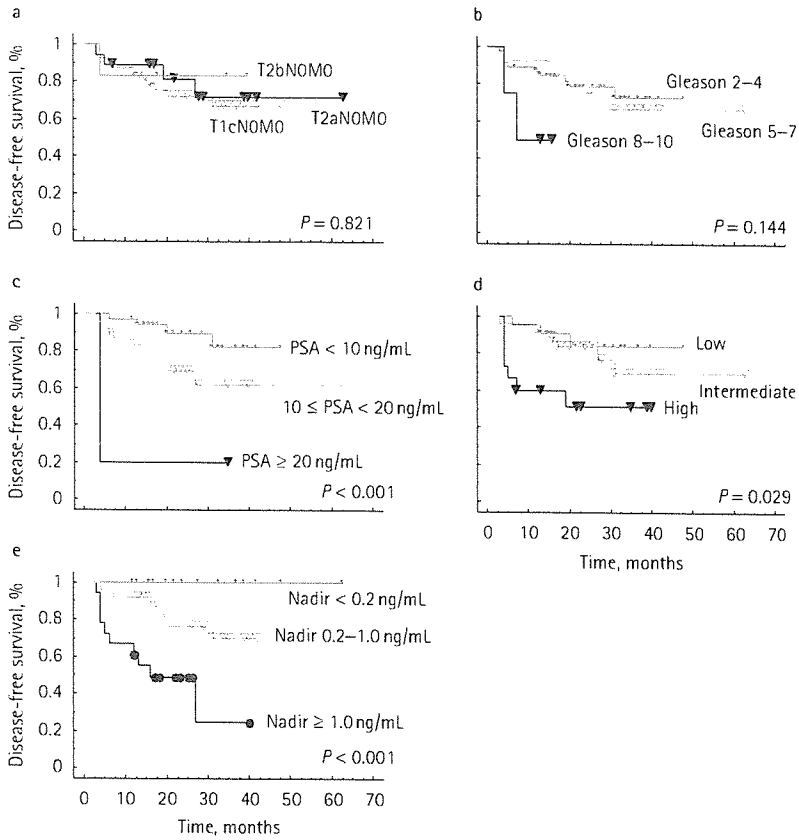

cancer. In 1996, Gelet *et al.* [18,19] reported a preliminary experience of HIFU using Ablatherm prototype 1.0 (EDAP-Technomed, Lyon, France) for treating localized prostate cancer. They later summarized their clinical outcome, in which there was a complete response in two-thirds of the patients, with no residual cancer and no three consecutive increases in PSA level. More recently, Chaussy and Thuroff [20] reported that the combination of TURP immediately before HIFU reduced the treatment-related morbidity, e.g. catheter time, incontinence, urinary infection and the IPPS. In addition, they summarized the clinical outcome using the ASTRO definition, an 84% stability rate in the HIFU group and an 80% rate in the TURP and HIFU group. In 1999, Beerlage *et al.* [21] reported results of 143 HIFU treatments using the Ablatherm prototype 1.0 and 1.1 in 111 patients with clinical stage T1–3N0M0 prostate cancer and a PSA level of <25 ng/mL. The first 65 treatments in 49 patients were selective (i.e. a unilateral or bilateral treatment in one or two sessions, depending on the findings from TRUS and biopsies) and the second 78 treatments in 62 patients treated the whole prostate. There was a complete response (defined as a PSA level of <4.0 ng/mL and a negative biopsy) in 60% of the group with the whole prostate treated, and in 25% of the selectively treated patients. In the present study, two patients who were treated selectively in the right lobe of the prostate for adenocarcinoma, identified by a prostate biopsy, showed a gradual increase in PSA level and viable cancer cells in the untreated lobe on prostate biopsy after HIFU. A second HIFU treatment of the whole prostate maintained the PSA at a low level, with a negative biopsy. Recently, many methods of imaging have been analysed for detecting prostate cancer, including TRUS, CT, endorectal coil MRI and multiple biopsies of the prostate under TRUS guidance. However, prostate cancer is a multifocal disease and it is not yet possible to determine the sites of microscopic foci of cancer cells by imaging analysis alone. Therefore, the whole prostate must be treated, as corroborated by the results of the present study and others.

When summarising the present clinical outcome by the ASTRO definition, 75% of the patients were biochemically disease-free. Particularly those patients whose PSA level before HIFU was <10 ng/mL and with a PSA nadir of <0.2 ng/mL had an 82% and 100% biochemical DFS rate at 3 years after HIFU treatment. In addition, the PSA nadir ($P < 0.001$) was a significant independent predictor of time to biochemical recurrence in the multivariate analysis.

HIFU treatment with the Sonablate machine is limited to a prostate size of 50 mL with the present device, even when using a longer focal-length probe. It is necessary to develop a longer focal-length probe for treating prostates of >50 mL. Neoadjuvant androgen-deprivation therapy may be useful in larger prostates to reduce the volume of the prostate before HIFU.

After HIFU there were urethral strictures at or near the verumontanum in the prostatic urethra in a quarter of the present patients, treated by internal urethrotomy and/or periodic dilatation with metal sounds. Using TURP after HIFU treatment may be useful to prevent urethral stricture or urinary retention [22,23]. A recto-urethral fistula occurred in one patient after the second HIFU treatment. More precise HIFU power control during repeat treatment is needed. A continuous cooling device was applied to keep the rectal mucosa at <18 °C during the procedure, and there was no recto-urethral fistula in any of the patients after using the automatic cooling system.

Generally, the radicality of prostate cancer and preservation of sexual function are always controversial because erectile dysfunction after treatment depends on preserving the neurovascular bundles that are sometimes invaded by the tumour. In the present study, 25% of the patients had erectile dysfunction after HIFU therapy; interestingly, two of the eight affected and who desired treatment recovered with sildenafil citrate. We consider that this rate is lower than after RP [2–5]; obviously, further experience is required to confirm this important consideration.

Variable	Hazard ratio (95% CI)	P
Age	1.009 (0.933–1.091)	0.825
Preoperative PSA	1.025 (0.961–1.093)	0.459
Stage	0.537 (0.218–1.320)	0.175
Gleason score	1.037 (0.635–1.641)	0.877
Prostate volume	0.968 (0.916–1.032)	0.256
PSA nadir	1.543 (1.208–1.973)	<0.001

TABLE 2
The Cox proportional hazards analysis predicting the time to biochemical failure after HIFU

Complications	N patients (%)	Treatment
Urethral stricture	15 (24)	Bougie or urethrotomy
Retrograde ejaculation	2 (3)	No treatment
Epididymitis	2 (3)	Antibiotics
Retention for 3 weeks	1 (2)	TURP
Stress incontinence (grade 1)	1 (2)	1 pad/day
Recto-urethral fistula	1 (2)	Colostomy and closure
Erectile dysfunction	8/34 (25)	Medical treatment

TABLE 3
The complications after HIFU

The median hospital stay in the present series was 4 days; this was related to local socio-economic conditions rather then clinical or technical factors. There is a significant difference in the national insurance systems between Japan and other countries. Usually, 20–30 days of hospitalization is recommended after RP in Japan. However, recent HIFU treatments at our hospital have involved only an overnight stay.

For many reasons, transrectal HIFU appears to be highly attractive as a minimally invasive treatment for localized prostate cancer. With HIFU treatment there is no incision or puncture, it is bloodless, can be delivered on an outpatient basis and is repeatable. It can also be used on patients with local recurrences who have already been treated with RP, cryoablation of the prostate and radiation therapy. In addition, the option of HIFU may be more attractive to the patient who wants to avoid incontinence and erectile dysfunction afterward, to maintain their quality of life. These features, combined with the optional curative effect, provide an ideal treatment for patients with localized prostate cancer. The few patients and the relatively short follow-up in the present series limit any definitive conclusions. We think that the present data suggest that HIFU has considerable potential as a noninvasive treatment for patients with localized prostate cancer.

ACKNOWLEDGEMENTS

The authors express their appreciation to Mr Y. Shimazaki, S. Kagosaki, K. Yamashita, K. Takai and N.T. Sanghvi for their technical assistance.

CONFLICT OF INTEREST

None declared.

REFERENCES

1 **Landis SH, Murray T, Bolden S, Wingo PA.** Cancer statistics, 1999. *CA Cancer J Clin* 1999; **49**: 8–31
2 **Arai Y, Egawa S, Tobisu K *et al.*** Radical retropubic prostatectomy: time trends, morbidity and mortality in Japan. *BJU Int* 2000; **85**: 287–94
3 **Catalona WJ, Smith DS.** Cancer recurrence and survival rate after anatomic radical retropubic prostatectomy for prostate cancer: intermediate-term results. *J Urol* 1998; **160**: 2428–34
4 **Han M, Walsh PC, Partin AW, Rodriguez R.** Ability of the 1992 and 1997 American Joint Committee on Cancer Staging for prostate cancer to predict progression-free survival after radical prostatectomy for stage T2 disease. *J Urol* 2000; **164**: 89–92
5 **Hull GW, Rabbani F, Abbas F, Wheeler TM, Kattan MW, Scardino PT.** Cancer control with radical prostatectomy alone in 1,000 consecutive patients. *J Urol* 2002; **167**: 528–34
6 **Vicini FA, Kini VR, Edmundson G, Gustafson GS, Stromberg J, Martinez A.** A comprehensive review of prostate cancer brachytherapy: defining an optional technique. *Int J Radiat Oncol Biol Phys* 1999; **44**: 483–91
7 **Han KR, Cohen JK, Miller RJ *et al.*** Treatment of organ confined prostate cancer with third generation cryosurgery: preliminary multicenter experience. *J Urol* 2003; **170**: 1126–30
8 **Zelefsky MJ, Wallner KE, Ling CC *et al.*** Comparison of the 5-year outcome and morbidity of three-dimensional conformal radiotherapy versus transperineal permanent iodine-125 implantation for early stage prostate cancer. *J Clin Oncol* 1999; **17**: 517–22
9 **Beerlage HP, Thuroff S, Madersbacher S *et al.*** Current status of minimally invasive treatment options for localized prostate carcinoma. *Eur Urol* 2000; **37**: 2–13
10 **Guillonneau B, el-Fettouh H, Baumert H *et al.*** Laparoscopic radical prostatectomy: oncological evaluation after 1,000 cases a Montsouris experience. *J Urol* 2003; **169**: 1261–6
11 **Uchida T, Sanghvi NT, Gardner TA *et al.*** Transrectal high-intensity focused ultrasound for treatment of patients with stageT1b-2N0M0 localized prostate cancer: a preliminary report. *Urology* 2002; **59**: 394–9
12 **Uchida T, Tsumura H, Yamashita H *et al.*** Transrectal high-intensity focused ultrasound for treatment of patients with stageT1b-2N0M0 localized prostate cancer: a preliminary report. *Jpn J Endourol ESWL* 2003; **16**: 108–14
13 **Wu JS, Sanghvi NT, Phillips MH *et al.*** Experimental studies using a split beam transducer for prostate cancer therapy in comparison to a single beam transducer. *IEEE Ultrasonics Symp Proc* 1999; **2**: 1443–6
14 **Madersbacher S, Pedevilla M, Vingers L, Susani M, Merberger M.** Effect of high-intensity focused ultrasound on human prostate cancer *in vivo*. *Cancer Res* 1995; **55**: 3346–51
15 **International Union Against Cancer: Sobin LH, Witterkind CH eds,** *TNM Classification of Malignant Tumors*, 5th

edn. New York: John Wiley and Sons, Inc. 1997: 170–3
16 **ASTRO.** Consensus statement. Guidelines for PSA following radiation therapy. American Society for Therapeutic Radiology and Oncology Consensus Panel. *Int J Radiat Oncol Biol Phys* 1997; **37**: 1035–41
17 **Zelefsky MJ, Hollister T, Raben A *et al.*** Five-year biochemical outcome and toxicity with transperineal CT-planned permanent I-125 prostate implantation for patients with localized prostate cancer. *Int J Radiat Oncol Biol Phy* 2000; **47**: 1261–6
18 **Gelet A, Chaperon JY, Bouvier R *et al.*** Treatment of prostate cancer with transrectal focused ultrasound: early clinical experience. *Eur Urol* 1996; **29**: 174–83
19 **Gelet A, Chapelon JY, Bouvier R, Rouviere O, Lyonnet D, Dubernard JM.** Transrectal high-intensity focused ultrasound for the treatment of localized prostate cancer: factors influencing the outcome. *Eur Urol* 2001; **40**: 124–9
20 **Chaussy CG, Thüroff S.** The status of high-intensity focused ultrasound in the treatment of localized prostate cancer and the impact of a combined resection. *Curr Urol Rep* 2003; **4**: 248–25
21 **Beerlage HP, Thuroff S, Debruyne FM, Chaussy C, de la Rosette JJ.** Transrectal high-intensity focused ultrasound using the Ablatherm device in the treatment of localized prostate carcinoma. *Urology* 1999; **54**: 273–7
22 **Blana A, Walter B, Rogenhofer S, Wieland WF.** High-intensity focused ultrasound for the treatment of localized prostate cancer: 5-year experience. *Urology* 2004; **63**: 297–300
23 **Vallancien G, Prapotnich D, Cathelineau X, Baumert H, Rozet F.** Transrectal focused ultrasound combined with transurethral resection of the prostate for the treatment of localized prostate cancer: feasibility study. *J Urol* 2004; **171**: 2265–7

Correspondence: Toyoaki Uchida, Department of Urology, Tokai University Hachioji Hospital, 1838, Ishikawa-machi, Hachioji, Tokyo 192–0032, Japan.
e-mail: tuchida@green.ocn.ne.jp

Abbreviations: **HIFU**, high-intensity focused ultrasound; **RP**, radical prostatectomy; **DFS**, disease-free survival; **ASTRO**, American Society for Therapeutic Radiology and Oncology.

Smoking Influences Aberrant CpG Hypermethylation of Multiple Genes in Human Prostate Carcinoma

Hideki Enokida, M.D., Ph.D.[1,2]
Hiroaki Shiina, M.D., Ph.D.[3]
Shinji Urakami, M.D., Ph.D.[1,3]
Masaharu Terashima, M.D., Ph.D.[4]
Tatsuya Ogishima, M.D.[1]
Long-Cheng Li, M.D.[1]
Motoshi Kawahara, M.D., Ph.D.[2]
Masayuki Nakagawa, M.D., Ph.D.[2]
Christopher J. Kane, M.D.[1]
Peter R. Carroll, M.D.[1]
Mikio Igawa, M.D., Ph.D.[3]
Rajvir Dahiya, Ph.D., D.Sc.[1]

[1] Department of Urology, Veterans Affairs Medical Center and University of California, San Francisco, California.

[2] Department of Urology, Kagoshima University, Kagoshima, Japan.

[3] Department of Urology, Shimane University, Izumo, Japan.

[4] Department Biochemistry and Molecular Medicine, Shimane University, Izumo, Japan.

This study was supported by NIH Grants RO1CA101844, RO1AG21418, T32DK07790, and VA Merit Review and REAP grants.

Address for reprints: Rajvir Dahiya, Ph.D., D.Sc., Professor of Urology, Director of Urology Research Center (112F), University of California San Francisco and VA Medical Center, 4150 Clement Street, San Francisco, CA 94121; Fax: (415) 750-6639, E-Mail: rdahiya@urol.ucsf.edu

Received May 18, 2005; revision received June 24, 2005; accepted July 28, 2005.

BACKGROUND. Aberrant CpG methylation profiles of gene promoters and their correlation with advanced pathologic features have been well investigated in prostate carcinoma (PC). Several case–control and prospective studies have revealed a positive association between current smoking and PC. The authors hypothesized that smoking influences both progression and prognosis of PC through CpG hypermethylation of related genes.

METHODS. A total of 164 PC patients (52 current, 30 former, and 82 never smokers) and 69 benign prostatic hyperplasia (BPH) patients were examined by methylation-specific PCR (MSP) for 3 genes: adenomatous polyposis coli (*APC*), glutathione S-transferase pi (*GSTP1*), and multidrug resistance one (*MDR1*). The methylation status of representative samples was confirmed by bisulfite DNA sequencing analysis. The newly defined methylation score (M-score) of each sample is the sum of the corresponding log hazard ratio (HR) coefficients derived from multivariate logistic regression analysis for pathology (BPH vs. PC), and was related to clinical and pathologic outcome including smoking status.

RESULTS. The M-score was significantly higher in the current smokers than in never smokers ($P = 0.008$). Spearman rank correlation test demonstrated a significant correlation between pack-years smoked and M-score in PCs ($P = 0.039$). Significant correlation of the M-score methylation was observed with high pT category ($P < 0.001$), high Gleason sum ($P < 0.001$), high preoperative prostate-specific antigen (PSA) ($P = 0.041$), and advanced pathologic features. In addition, Gleason sum was significantly associated with PSA failure-free probability as a poor outcome ($P = 0.020$).

CONCLUSIONS. This is the first study to demonstrate significant correlation of the methylation status of multigenes with smoking status in PC. Smoking status may influence both progression and prognosis of PC through CpG hypermethylation of related genes. ***Cancer* 2006;106:79–86.** © *2005 American Cancer Society.*

KEYWORDS: smoking, methylation, *APC, GSTP1, MDR1*, human prostate carcinoma, prostate cancer.

Prostate carcinoma (PC) is one of the most common malignancies among men.[1] Smoking is strongly associated with cancers of the head and neck, esophagus, lung, and urinary bladder.[2] Several potential mechanisms whereby smoking may increase risk of PC involve male hormones or cadmium.[3–5] Aberrant methylation profiles of gene promoters and their correlation with advanced pathologic features have been well investigated in PC.[6–8] In lung cancers, some investigators have previously reported that there were significant correlations between aberrant promoter methylation of genes and smoking status of patients.[9–12] However, such studies in PC are lacking in the literature.

Several case–control studies have revealed a positive association

DOI 10.1002/cncr.21577
Published online 1 December 2005 in Wiley InterScience (www.interscience.wiley.com).

between current smoking and PC.[3,13–18] Previous reports also have demonstrated an association between smoking and advanced PC.[3,17–19] Furthermore, the majority of prospective studies that used PC death as an outcome noted positive association between current smoking and PC.[4] Recent studies from our laboratory have shown that methylation analysis of the *APC, GSTP1, and MDR1* genes correlate with progression of prostate carcinoma.[20,21] When several genes are analyzed in the same samples, careful interpretation of the results is necessary because each gene or other clinical factors, including age, may influence one another.[22,23] We hypothesize that smoking influences both progression and prognosis of PC through CpG hypermethylation of related genes. To test this hypothesis, we used a methylation score (M-score) that is the sum of the log of the hazard ratios (HR) for each gene, analyzed by multivariate logistic regression analysis for pathology (benign prostatic hyperplasia [BPH] vs. PC). We also related the M-score to clinical and pathologic outcome, including smoking status. In addition, we assessed prostate specific antigen (PSA) failure-free probability against the clinicopathologic features of PC.

TABLE 1
Clinicopathologic Characteristics of Prostate Carcinoma according to Smoking Status

		Smoking			
	Overall	Current smokers	Former smokers	Never smokers	*P* value
Total no.	164	52	30	82	0.154
Median age (range)	69 (49–87)	68 (49–80)	71 (62–78)	69 (51–80)	0.154
Smoke exposure					
Pack-yrs smoked[a]	40 ± 26	42 ± 24	37 ± 30	—	
Yrs smoked	40 ± 11	44 ± 8	34 ± 13	—	
Starting age	23 ± 8	23 ± 7	23 ± 10	—	
pT category					
pT1	0	0	0	0	0.590
pT2	108	31	21	56	
pT3	52	20	9	23	
pT4	4	1	0	3	
Gleason sum					
< 7	82	23	19	40	0.495
7	53	20	7	26	
> 7	29	9	4	16	
Preoperative serum PSA					
< 4	22	4	6	12	0.611
≥ 4, < 10	77	26	13	38	0.611
≥ 10	65	22	11	32	

PSA: prostate - specific antigen.
There are no significance differences in clinical backgrounds such as age, pT category, Gleason sum, and preoperative PSA among smoking statuses.
[a] Pack-years smoked is years smoked × cigarettes per day/20.

MATERIALS AND METHODS

Tissue Samples

A total of 164 newly diagnosed PC tissues from radical prostatectomies and 69 pathologically proven BPH samples from transurethral resection (TUR-P) were obtained from Shimane University Hospital (Izumo, Japan). The patients' clinicopathologic characteristics including their smoking status are summarized in Table 1. Each tumor was graded and staged according to the Gleason grading system and the TNM staging system.[24,25] Current smokers were defined as those who smoked within 12 months of tumor development. Former smokers were those who had quit smoking more than 12 months before tumor development. None of these patients had received androgen deprivation therapy before radical prostatectomy. We used serum PSA levels after radical prostatectomy as a surrogate end-point, with a level equal to or above 0.2 ng/mL designated as PSA failure. Forty-five patients with PC were excluded from the PSA failure-free probability study because of adjuvant hormonal therapy immediately after radical prostatectomy. PSA failure-free probability was determined as the percentage of patients without PSA failure. Follow-up ranged from 0.7 to 91.4 months, with a median of 33.9 months.

Tissue Preparations

All samples were fixed in 10% buffered formalin (pH 7.0) and embedded in paraffin wax. For histologic evaluation, 5 μm-thick sections were used for hematoxylin and eosin (H & E) staining. All samples were microscopically dissected and analyzed for methylation.[26] In BPH samples, the presence of high-grade prostate intraepithelial neoplasia (PIN) and carcinoma were ruled out by microscopic analysis.

Nucleic acid extraction

Genomic DNA from all prostate samples was extracted using a commercial kit (Qiagene, Valencia, CA), and precipitated with ethanol. The concentration of DNA was determined with a spectrophotometer, and its integrity was checked by gel electrophoresis.

Methylation Analysis

Genomic DNA from all prostate samples (100 ng) was subjected to sodium bisulfite modification using a CpGenome DNA Modification Kit (Intergen Co., Purchase, NY). Based on the functional promoter sequence of *APC*,[27] methylation-specific polymerase chain reaction (MSP) and unmethylation-specific polymerase chain reaction (USP) primers were designed by using MethPrimer software (http://itsa.ucsf.